Experimental and numerical modeling of rarefied gas flows through orifices and short tubes

S.F. Gimelshein*, G.N. Markelov†, T.C. Lilly*, N.P. Selden* and A.D. Ketsdever**

*University of Southern California, Los Angeles, CA 90089
†Advanced Operations and Engineering Services, The Netherlands
**Air Force Research Laboratory, Edwards AFB, CA 93524

Abstract. Flow through circular orifices with thickness-to-diameter ratios varying from 0.015 to 1.2 is studied experimentally and numerically with kinetic and continuum approaches. Helium and nitrogen gases are used in the range of Reynolds numbers from 0.02 to over 700. Good agreement between experimental and numerical results is observed for mass flow and thrust corrected for the experimental facility background pressure. For thick-to-thin orifice ratios of mass flow and thrust *vs* pressure, a minimum is established. The thick orifice propulsion efficiency is much higher than that of a thin orifice. The effects of edge roundness and surface specularity on a thick orifice specific impulse were found to be relatively small.

INTRODUCTION

Rarefied gas flows through circular orifices and short and long tubes have been studied extensively in the past. Free molecular and transitional flow in tubes and ducts was first studied experimentally and theoretically by Knudsen [1] who examined the dependence of the conductance at different pressure and geometrical parameters. He observed a conductance minimum at $Kn \approx 1$ for long ducts and tubes. A qualitative explanation for conductance minimum was suggested in [2]. The minimum was attributed to a small population of molecules that enter the tube or reflect on the tube surface with a very small radial velocity. These molecules give a disproportionately large contribution to the mass flow at high Knudsen numbers. As the Knudsen number decreases, molecular collisions disrupt the path of such molecules, therefore decreasing the mass flow. Further increase in the molecular collision frequency results in an overall drift velocity that in turn increases the mass flow through the tube.

The conductance and the transmission probabilities in long tubes and channels in the transitional flow has been extensively studied in the 1960s and 1970s, both experimentally [3] and analytically [4]. There were also quite a few studies aimed at flows through short tubes and apertures [5, 6]. Examples of such studies are [7] where the effect of round edges on mass flow was analyzed, and [8] where empirical fits were suggested for conductance of sharp-edged orifices and rectangular ducts. This type of flow was also investigated in detail in the past decade, most noticeably with respect to emerging micro and nanotechnologies (such as lubrication problems that deal with transitional flows in long channels and tubes) and porous media (represented by a single or multiple capillaries). Although many researchers have made significant contribution to the field, we mention here only [9, 10, 11].

Although an extensive knowledge has been accumulated on transitional flows in orifices and short tubes, there have been few investigations of orifice/tube that concentrate on momentum flux (or thrust) and specific impulse [12, 13]. The main goal of this work is to study experimentally and numerically the above parameters of thin-walled orifice and short circular tube geometries, and perform a comparatative analysis for different tube length and edge bluntness in a wide range of Reynolds numbers from free molecular to near-continuum regime. The study also extends the low end of the Reynolds number range that previous studies have investigated by extending operating conditions down to the free molecule flow regime.

The experiments and computations were conducted at room temperature, used nitrogen and helium as test gases and varied the stagnation pressure from several millitorr to about 40 torr. The computations are performed using two different approaches: a kinetic approach (the direct simulation Monte Carlo method, DSMC) and a continuum approach (solution of the Navier-Stokes equations, NS hereafter).

CP762, *Rarefied Gas Dynamics: 24th International Symposium,* edited by M. Capitelli

Report Documentation Page

Form Approved
OMB No. 0704-0188

1. REPORT DATE	2. REPORT TYPE	3. DATES COVERED
13 JUL 2005	**N/A**	**-**

4. TITLE AND SUBTITLE
Experimental and numerical modeling of rarefied gas flows through orices and short tubes

5a. CONTRACT NUMBER
5b. GRANT NUMBER
5c. PROGRAM ELEMENT NUMBER

6. AUTHOR(S)

5d. PROJECT NUMBER
5e. TASK NUMBER
5f. WORK UNIT NUMBER

7. PERFORMING ORGANIZATION NAME(S) AND ADDRESS(ES)
University of Southern California, Los Angeles, CA 90089

8. PERFORMING ORGANIZATION REPORT NUMBER

9. SPONSORING/MONITORING AGENCY NAME(S) AND ADDRESS(ES)

10. SPONSOR/MONITOR’S ACRONYM(S)

11. SPONSOR/MONITOR’S REPORT NUMBER(S)

12. DISTRIBUTION/AVAILABILITY STATEMENT
Approved for public release, distribution unlimited

13. SUPPLEMENTARY NOTES
See also ADM001792, International Symposium on Rarefied Gas Dynamics (24th) Held in Monopoli (Bari), Italy on 10-16 July 2004.

14. ABSTRACT

15. SUBJECT TERMS

16. SECURITY CLASSIFICATION OF:			17. LIMITATION OF ABSTRACT	18. NUMBER OF PAGES	19a. NAME OF RESPONSIBLE PERSON
a. REPORT	b. ABSTRACT	c. THIS PAGE			
unclassified	**unclassified**	**unclassified**	**UU**	**7**	

Standard Form 298 (Rev. 8-98)
Prescribed by ANSI Std Z39-18

EXPERIMENTAL SET UP AND FLOW CONDITIONS

All thrust measurements were performed on the nano-Newton Thrust Stand (nNTS) which has been described in detail by Jamison, et. al [14] and specially modified for this experiments specific needs. The nNTS was installed in Chamber IV of the Collaborative High Altitude Flow Facilities (CHAFF-IV) which is a 3 m diameter by 6 m long cylindrical, high vacuum chamber. The facility was pumped with a 1 m diameter diffusion pump with a pumping speed of 42,000 L/s for helium and 25,000 L/s for molecular nitrogen in conjunction with a Turbomolecular pump with a pumping speed of 3,500 L/s for molecular nitrogen. The ultimate facility pressure was approximately 10^{-6} Torr with all operational pressures below 10^{-3} Torr. Measurements of the chamber background pressure were taken with an absolute pressure transducer in conjunction with an ionization gauge.

The thickness of the orifice, t, was varied from 0.015 mm to 1.2 mm, while the diameter d was constant at 1mm. All geometries tested experimentally were sharp edged. The orifice was attached to a plenum with a cross-sectional area much larger than the orifice area to help ensure uniform flow. The thinnest orifice was machined in a 0.015 mm thick tantalum shim giving $t/d = 0.015$. This geometry was chosen to minimize the viscous effects in the orifice flow. The medium and thickest walled orifices were both 1 mm in diameter and machined into aluminum plates of respective thicknesses to give t/d values of 0.58 and 1.2, respectively. The plenum size (66x35x17.5 mm) is the same for all orifices. The stagnation pressures for all three orifices were measured through taps on the side of the plenums using calibrated differential pressure transducers. The propellant was introduced to the plenum through an adjustable needle valve located downstream of a mass flow meter. In the experimental configuration, the mass flow meters were operated in the continuum regime throughout the pressure range investigated. The propellants used were molecular nitrogen and helium. The stagnation pressures ranged from several hundred milliTorr to approximately 40 Torr. The stagnation temperature was measured to be 295 K in equilibrium with ambient.

The nNTS was calibrated using electrostatic calibration techniques described by Selden and Ketsdever [15]. A unique feature of the nNTS is its ability to measure the force levels of the 1.0 mm orifice from the free molecule through continuum range. The low thrust measuring capability of the nNTS allowed for the investigation of the transitional flow regime overlooked in previous low Reynolds number studies.

NUMERICAL APPROACHES

Kinetic approach. The DSMC-based software system SMILE [16] was used in all DSMC computations. The important features of SMILE that are relevant to this work are parallel capability, different collision and macroparameter grids with manual and automatic adaptations, and spatial weighting for axisymmetric flows.

The majorant frequency scheme [17] was used to calculate intermolecular interactions. The intermolecular potential was assumed to be a variable hard sphere [18]. Energy redistribution between the rotational and translational modes was performed in accordance with the Larsen-Borgnakke model. A temperature-dependent rotational relaxation number was used. The reflection of molecules on the surface was assumed to be diffuse with complete energy and momentum accommodation. Zero flow velocity was assumed at the inflow boundaries, with the number flux and temperature corresponding to given stagnation conditions.

Continuum approach. The Navier-Stokes computations were performed with commercial software, CFD-FASTRAN, which is a sophisticated compressible finite-volume flow solver [19]. The software is designed to simulate steady and unsteady flows, perfect gas and multispecies reacting flows, and has advanced features such as 6-DOF modeling for simulating the unsteady dynamic motion of multi-body configurations.

The following features of CFD-FASTRAN are used for present computations. structured grid solver; Roe's approximate Riemann solver as a flux difference scheme with minmod limiter to allow up to second order accuracy; implicit scheme with local time stepping; Sutherland law for the viscosity.

RESULTS AND DISCUSSION

Flowfield structure and comparison of kinetic and continuum approaches. The use of kinetic and continuum approaches for the higher pressures under consideration not only provides more information on the flow, but also allows us to address the accuracy issues for the numerical solutions. It is well known that the Boltzmann equation, and therefore the DSMC method, is applicable well above the range of pressures considered in this work. The use of the DSMC method for modeling very low Knudsen number flows (of the order of 0.001), however, is still raising questions related to the numerical accuracy of obtained solutions, primarily related to the number of simulated molecules and cells. This is further magnified by uncertainty in the subsonic boundary conditions, as well as the long time required to reach steady state. The solution of the NS equations, on the other hand, is limited by its area of applicability. In application to this work, the NS equations are applicable only for a higher range of pressures considered. The lowest Reynolds number for which these equations were solved is 290, and the breakdown parameter field [18] for this case is shown in Fig. 1.

Comparison of the number density normalized by the stagnation value calculated with DSMC and NS is given in Fig. 2 for the thin orifice case ($t/d = 0.015$) with a stagnation pressure of 5,200 Pa in helium. The agreement is very good between the continuum and kinetic approaches in the core flow, except for a small region near the axis. The NS contours are artificially curved there, coming to the axis at angles different from 90 deg. For larger angles from the axis, however, there is a large difference (see Fig. 3). This difference is attributed to the no-slip boundary conditions used in NS and very high degree of flow rarefaction (and therefore thermal nonequilibrium). The difference is especially noticeable in all temperature-dependent properties, but is also visible for such a important parameter as axial velocity. Comparison of DSMC and NS axial velocity contours given in Fig. 4 shows, however, that the radial velocities in the vicinity of the exit are very close for the two methods.

The axial velocity field for the thick tube ($t/d = 1.2$) is shown in Fig. 5. There is a relatively thick boundary layer inside the tube. Whereas the axial velocity at the tube entrance is close to that at the thin orifice exit plane, the gas strongly accelerates along the tube, resulting in exit values almost two times as high. Again, the values near the outer surface are significantly different for the two approaches due to the reasons stated above.

Comparison of numerical and experimental data. The experimental and computational mass flow through an orifice ($t/d = 0.015$) at different stagnation pressures is compared for two gases in Fig. 6. As expected, the mass flow increases almost linearly for the presented range of pressures. The most important fact is that there is a very good agreement, within one or two percent, between the measured mass flow and that obtained with the DSMC. The difference is negligibly small for the entire range of pressure values both for helium and nitrogen. The continuum approach somewhat underpredicts the data (see previous section).

Comparison of the thrust results for this case is shown in Fig. 7. It is seen that the modeling (both DSMC and NS) overpredicts the experimental data, with difference amounting to about 10 percent for high pressures. While there can be several possible reasons for such a difference, including numerical and experimental uncertainties, the most important one is the impact of the background pressure. A small but finite background pressure was always present in the experiments, although it was not included in simulations. The impact of the background molecules is indirect, and related to the plume shadowing of the front (containing the orifice) side of the plenum [20]. Plume molecules expand from the orifice and collide with background molecules, thus prohibiting these molecules from colliding with the plenum front surface. As a result, the background gas pressure on the front surface may decrease drastically, while the background pressure on the back surface of the plenum is not affected by the plume. Even though the background pressure is about 0.003 percent of that in the plenum, the ratio of the plenum back surface area to the orifice area is about 3,000. This may cause a decrease in the total force on the order of 10 percent. The experimental values for thrust were corrected using the actual background surface pressure force assuming that all background gas was removed near the plenum front surface. The corrected data is shown as error bars on the measured thrust in Fig. 7. Note that there is a very good agreement between the computed and experimental (corrected) force for the entire range of pressures under consideration, thus suggesting that background pressure was the main source of the difference.

Comparison between the measured and computed mass flow for medium and thick orifice configurations is given in Figs. 8 and 9. Since the dependence of mass flow and force on the orifice thickness will be analyzed in the following section, here we mention only that the agreement between the data and the computations is very good for $t/d = 0.58$ and $t/d = 1.2$. The dependence of the mass flow on pressure is noticeably non-linear, especially for $t/d = 1.2$. The DSMC method captures the corresponding curvature rather accurately for the two propellants. Another important conclusion is that the fully diffuse surface accommodation model, used in the DSMC method, appears to be quite adequate for the mass flow prediction.

The experimental and numerical values of thrust for the thickest orifice are plotted in Fig. 10. The experimental data are somewhat smaller than the numerical results; however, they are higher when corrected for the background pressure. This may be due to a relative transparency of the plume for background molecules at lower pressures, which means that only a part of the background pressure needs to be included.

Impact of t/d ratio on mass flow and force. The ratios of mass flow and force values obtained for t/d of 0.58 and 1.2 using the DSMC method to those for $t/d = 0.015$ are presented in Fig. 11 for helium. Both mass flow and force ratios generally decrease with pressure for pressures ranging from nearly continuum regime down to $P \approx 100$ Pa, which correspond to a Knudsen number of about 0.25. The decrease is more pronounced for the larger t/d ratio. There is a minimum observed both for mass flow and force ratios at pressures between 50 and 100 Pa ($0.25 < Kn < 0.5$). After that, the ratio increase slightly towards the free molecular regime.

The ratio minimum is very small, about 1 percent, for the mass flow ratio, and much larger, up to 10 percent, for the force ratio. This means that the orifice efficiency in the above pressure range will be worse for the thick orifice compared to the thin one. The qualitative explanation for the minimum is somewhat similar to that for the Knudsen minimum effect, cited in the introduction. Let us first compare the flow though a thin and a thick orifice in the free molecular regime. Practically all molecules that intersect the orifice plane leave the plenum for $t/d = 0.015$ (only about 1.5% of the total number of intersecting molecules will return back to the plenum). For a thick orifice, however, the transmission probability may be much lower than unity, depending on t/d ratio, which explains much lower mass flows in this regime.

As Knudsen number decreases, the effect of collisions inside a thicker orifice becomes significant. This effect for relatively high Knudsen numbers results in decrease in mass flow since molecules that have relatively high axial velocities and whose contribution to mass flow is highest now have a finite probability to collide with molecules that previously collided with the tube surface. The contribution of these high axial velocity molecules therefore goes down as their axial velocity decreases after such collisions. The further decrease in the Knudsen number results in a general drift of molecules downstream towards the exit due to intermolecular collisions. The overall drift velocity increases as the boundary layer inside the tube decreases, thus forcing mass flow and force values to approach the corresponding thin orifice values. The experimental mass flow ratio of the thicker to the thinner orifice is also presented in Fig. 11. The agreement between the data and DSMC results is good, although the scatter of the data is relatively high, and it is not possible to clearly identify the minimum in the ratio.

Specific impulse. The impact of orifice shape and accommodation coefficient on gas flow fields and mass and momentum fluxes has also been studied. Only the DSMC method was utilized in this study. Comparison of the axial velocity contours for a straight and rounded (radius of curvature is $R = 0.29d$) geometric configurations is shown in Fig. 12. Note that the difference is rather small and observed primarily near the inner and outer edges.

The effect of surface specularity is shown in Fig. 13 where the normalized density and axial velocity profiles are given along the exit of the thickest orifice for a fully diffuse model ($\alpha_D = 1$) and a Maxwell model with $\alpha_D = 0.8$ (80% of molecules are reflected diffusely, and 20% are reflected specularly). An interesting fact is that surface specularity primarily affects the density field, and not the axial velocity. Axial velocity for the two α_D parameters almost coincide except for a small region near the surface where the velocity of the more specular case is higher. The number density however is proportionally lower for $\alpha_D = 0.8$ at any location at the orifice exit.

The orifice specific impulse results obtained with the DSMC method are summarized in Table 1. Several conclusions can be drawn from these results. First, for Knudsen numbers up to 0.05 the orifice efficiency for medium and thick orifice configurations are significantly larger than those for a thin orifice. For higher pressures, however, the orifice thickness has little effect. Second, there is no considerable difference in the specific impulse between the medium and thick orifices. The effect of adding 20% surface specularity also does not change the orifice efficiency.

CONCLUSIONS

The results obtained with the continuum approach for a range of Reynolds numbers from 290 to 770 are in very good agreement with the DSMC predictions both in terms of the flow fields and mass and momentum fluxes. It was also shown that the numerical predictions of the mass flow are in good agreement with the experimental data for all plenum pressures under consideration and thickness-to-diameter ratio varying from 0.015 to 1.2. However, the computed thrust was found to be up to ten percent higher than the experimental one. The difference is attributed to the impact of the background pressure that was not included in the computations. The data corrected for the background pressure agrees well with the numerical predictions.

The effect of the orifice thickness was studied, and a minimum was observed for thick-to-thin orifice ratios of mass flow and thrust *vs* pressure. The minimum occurs at a Knudsen number of about 0.25, and is about 1 percent lower than the free molecular value for the mass flow ratio, and about 10 percent lower than the corresponding force ratio. The

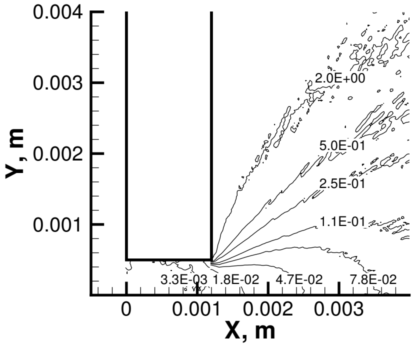

FIGURE 1. Breakdown parameter for t/d=1.2 computed by DSMC. Helium flow, $P_0 = 3,570$ Pa.

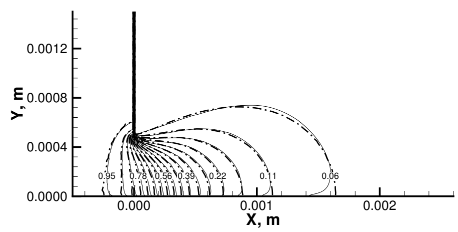

FIGURE 2. Normalized density fields for t/d=0.015. Helium flow, $P_0 = 5,200$ Pa. Solid lines, NS; dashed lines, DSMC.

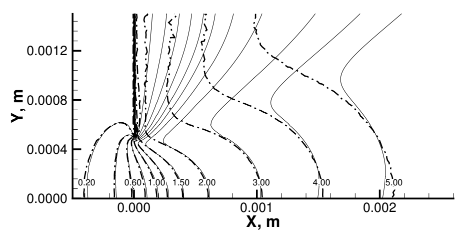

FIGURE 3. Mach number fields for t/d=0.015. Helium flow, $P_0 = 5,200$ Pa. Solid lines, NS; dashed lines, DSMC.

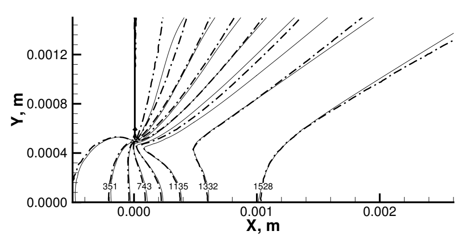

FIGURE 4. Axial velocity (m/s) fields for t/d=0.015. Helium flow, $P_0 = 5,200$ Pa. Solid lines, NS; dashed lines, DSMC.

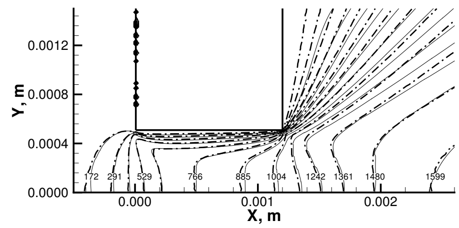

FIGURE 5. Axial velocity (m/s) fields for t/d=1.2. Helium flow, $P_0 = 5,200$ Pa. Solid lines, NS; dashed lines, DSMC.

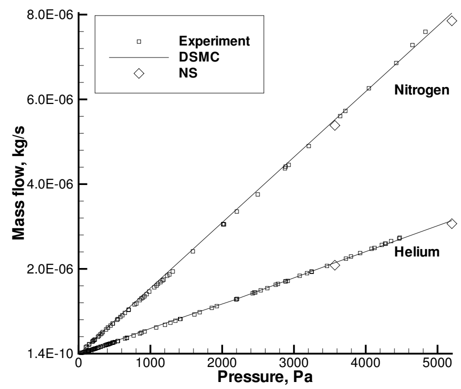

FIGURE 6. Comparison of experimental and numerical mass flow *vs* pressure for t/d=0.015 and two gases.

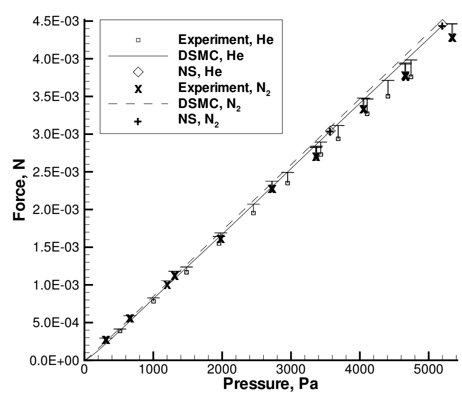

FIGURE 7. Comparison of experimental and numerical force *vs* pressure for t/d=0.015 and two gases.

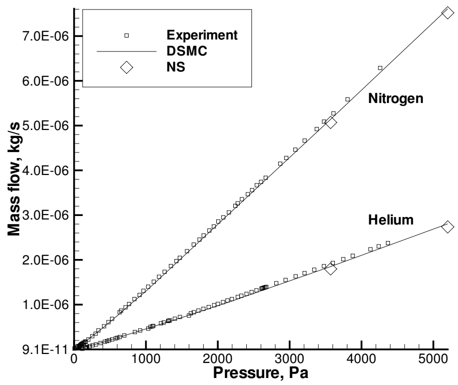

FIGURE 8. Comparison of experimental and numerical mass flow *vs* pressure for t/d=0.58 and two gases.

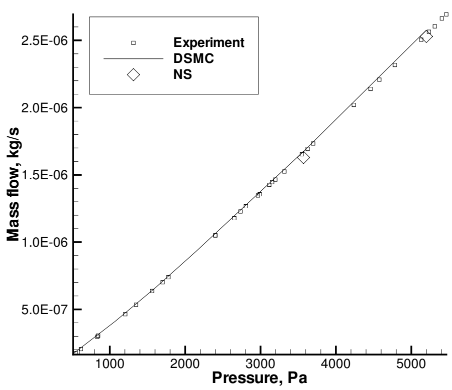

FIGURE 9. Comparison of experimental and numerical mass flow *vs* pressure for t/d=1.2 in helium.

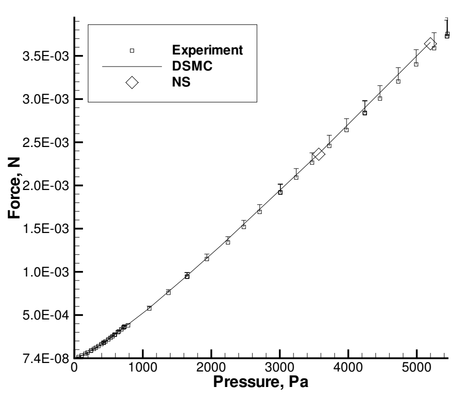

FIGURE 10. Comparison of experimental and numerical force *vs* pressure for t/d=1.2 in helium.

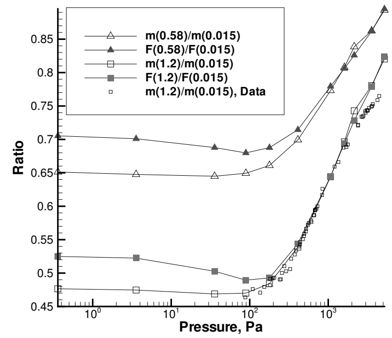

FIGURE 11. Thick-to-thin orifice mass flow and force ratio. Helium flow.

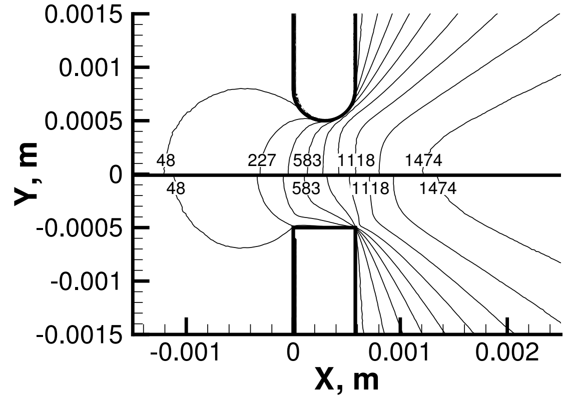

FIGURE 12. Axial velocity (m/s) fields for different shape of the orifice. Helium flow, t/d=0.58, $P_0 = 5,200$ Pa.

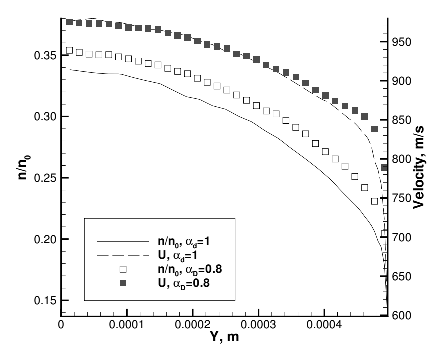

FIGURE 13. Normalized density and axial velocity (m/s) profiles at the orifice exit for $\alpha_D = 1$ and $\alpha_D = 0.8$. Helium, t/d=1.2, $P_0 = 410$ Pa.

qualitative explanation for the minimum is similar to that of the Knudsen minimum effect; namely, a disproportionally large contribution to mass flow and force from molecules with large axial and small radial velocities. This contribution decreases as these molecules collide with molecules reflected from the surface at the flow regime where intermolecular collisions are too rare for a collisional drift to be initiated.

The thick orifice specific impulse is much higher than that of a thin orifice, but does not change significantly when thickness-to-diameter ratio changes from 0.5 to 1. The effects of edge roundness and surface specularity on a thick orifice specific impulse were found to be relatively small.

ACKNOWLEDGMENTS

This work was supported in part by the Propulsion Directorate of the Air Force Research Laboratory at Edwards Air Force Base, California. GNM thanks Paul Pearson (AOES, Netherlands) for his help with computer resources for the NS computations, and Gerhard Boehmler (CFD RC, Germany) for providing a validation license of CFD-FASTRAN.

REFERENCES

1. Knudsen, M. *Annalen der Physik* (Leiptzig), 1909, Vol. 28, pp. 999-1016.
2. Pollard, W.G., Present, R.D. “On Gaseous Self-Diffusion in Long Capillary Tubes,” *Phys. Rev.*, 1948, Vol. 73, pp. 762-774.
3. Sreekanth, A.K. “Slip flow through long circular tubes,” 6th Symposium on Rarefied gas Dynamics, 1968, pp. 667-680.
4. Henning, H. *Vacuum'*, 1977, Vol. 28, No. 3, pp. 151-152.
5. Lord, R.G., Hurlbut, F.C., Willis, D.R. 6th Symposium on Rarefied gas Dynamics, 1968, pp. 1235-1243.
6. Sreekanth, A.K. *Phys. Fluids*, 1965, Vol. 8, No. 11, pp. 1951-1955.
7. Smetana, F.O., Sherrill, W.A., Schort, D.A. 6th Symposium on Rarefied gas Dynamics, 1968, pp. 1243-1257.
8. Kieser, J. Grundner, M. *Vide*, 1980, Vol. 201, p. 376.
9. Kaplan, C.R., Oran, E.S. 1999 Int. Conf. on Modeling and Simulation of Microsystems; Cambridge, MA, USA, 1999, p. 506-509.
10. Sharipov, F., Kalempa, D. *J. Vac. Sci. Technol. A,* 2002, Vol. 20, No. 3, pp. 814-822.
11. Bahukudumbi, P, Beskok, A. ‘*J. Micromech. Microeng.,* 2003, Vol. 13, pp. 873-884.
12. Ketsdever, A., Proc. 23rd International Symposium on Rarefied Gas Dynamics, ed. by A. Ketsdever and E.P. Muntz, American Institute of Physics, New York, 2002, pp. 1057-1064.
13. Alexeenko, A., Gimelshein, S., Levin, D., Ketsdever, A., and Ivanov, M., Journal of Propulsion and Power, Vol. 19, No. 4, 2003, pp. 588-594.
14. Jamison, A., Ketsdever, A., Muntz, E.P., *Review of Scientific Instruments,* Vol. 73, No. 10, 2002, pp. 3629-3637.
15. Ivanov, M., Markelov, G., Ketsdever, A., and Wadsworth, D., *AIAA Paper 99-0166,* January 1996.
16. Ivanov, M.S., Markelov, G.N., Gimelshein, S.F. *AIAA Paper 98-2669,* June 1998.
17. Ivanov, M.S., Rogasinsky, S.V., *Soviet J. Numer. Anal. Math. Modeling*, Vol. 3, No. 6, 1988, pp. 453-465.
18. Bird, G.A., *Molecular Gas Dynamics and the Direct Simulation of Gas Flows.* Clarendon Press, Oxford. 458 pp, 1994.
19. CFD-FASTRAN: User Manual, Version 2003, CFD Research Corporation (Huntsville, AL), 2003.
20. Ketsdever, A.D.. *J. Propulsion and Power,* 2002, Vol. 18, No. 4, pp. 797-804.
21. *Foundations of vacuum science and technology*, ed. by J.M. Lafferty, John Wiley & Sons, 1998.

TABLE 1. Orifice specific impulse for helium and different orifice thickness and plenum pressure values.

P, Pa	Kn	I_{sp} t/d=0.015	I_{sp} t/d=0.58	I_{sp} t/d=0.58 round	I_{sp} t/d=1.2	I_{sp} t/d=1.2 $\alpha_D = 0.8$
0.36	48.8263	102.5	111.0	1.112E+02	112.9	111.9
3.57	4.8826	102.9	111.4		113.3	
35.7	0.4883	108.2	115.4	1.166E+02	116.1	116.4
89.25	0.1953	115.2	120.6		120.0	
178.5	0.0977	122.8	127.7		125.0	
410.56	0.0425	131.6	134.4	1.374E+02	132.8	133.6
1071	0.0163	140.2	141.3		140.3	
1605.5	0.0109	143.5	143.2		143.0	
2142	0.0081	146.1	143.8		143.2	
3570	0.0049	144.6	144.5	1.459E+02	144.3	143.8
5200	0.0034	144.3	144.6		144.9	